# Kinetic magnetoelectric effect in a two-dimensional semiconductor strip due to boundary-confinement-induced spin-orbit coupling

Yongjin Jiang[1] and Liangbin Hu[2]
[1]*Department of Physics, Zhejiang Normal University, Jinhua, Zhejiang 321004, People's Republic of China*
[2]*Department of Physics and Laboratory of Photonic Information Technology, South China Normal University, Guangdong 510631, People's Republic of China*

(Received 28 March 2006; revised manuscript received 23 May 2006; published 1 August 2006)

In a thin strip of a two-dimensional (2D) semiconductor electronic system, spin-orbit coupling may be induced near both edges of the strip due to the substantial spatial variation of the confining potential in the boundary regions. In this paper we show that, in the presence of boundary-confinement-induced spin-orbit coupling, a longitudinal charge current circulating through a 2D semiconductor strip may cause *strong* nonequilibrium spin accumulation near both edges of the strip, and the nonequilibrium spin accumulation will be polarized perpendicular to the two-dimensional electron gas plane but along opposite directions at both edges of the strip. This phenomenon is essentially a kinetic magnetoelectric effect from the theoretical points of view, but it manifests in a very similar form as was conceived in a spin Hall effect.

DOI: 10.1103/PhysRevB.74.075302 PACS number(s): 72.25.−b, 75.47.−m

## I. INTRODUCTION

There has recently been much interest in a fascinating topic in the research community, namely the *spin Hall effect*. The spin Hall effect is such a phenomenon that a transverse spin current is generated when a longitudinal charge current circulates through a sample, and if the sample has a thin strip geometry, the transverse spin current will cause nonequilibrium spin accumulation at both edges of the strip.[1–3] Such a phenomenon would be attractive in the context of semiconductor spintronics since it might provide an effective way for generating spin currents and/or nonequilibrium spin density in a nonmagnetic semiconductor without the use of ferromagnetic metals or ferromagnetic semiconductors, a principal challenge in semiconductor spintronics.[4,5] From the theoretical points of view, such a phenomenon can arise from either *intrinsic* spin-orbit (SO) coupling (i.e., spin-orbit splitting of the band structure)[2,3] or *extrinsic* SO coupling (i.e., spin-orbit dependent impurity scatterings)[1,6] in a semiconducting material, and correspondingly, the phenomena due to intrinsic SO coupling were termed the *intrinsic spin Hall effect* and the phenomena due to spin-orbit dependent impurity scatterings termed the *extrinsic spin Hall effect*. From the standpoint of spintronic applications, the intrinsic spin Hall effect is more attractive since it is an intrinsic property of a semiconducting material and does not rely on spin-orbit dependent impurity scatterings.[2,3] Recently two experiments were reported on the observation of spin Hall effect. One is on *n*-doped bulk GaAs by Kato *et al.*[7] and the other is on two-dimensional *p*-doped GaAs by Wunderlich *et al.*[8] The phenomenon observed in two-dimensional *p*-doped GaAs by Wunderlich *et al.* was believed to be an intrinsic spin Hall effect since the edge spin accumulation detected in a thin strip of such a system is insensitive to impurity scatterings in the weak impurity scattering limit,[8] an important feature of the intrinsic spin Hall effect.[2,3] In contrast, the phenomenon observed in *n*-doped bulk GaAs by Kato *et al.* was believed to have an extrinsic origin (i.e., due to spin-orbit dependent impurity scatterings) since the edge spin accumulation detected in a thin strip of such a system is several orders of magnitude smaller compared with the theoretical predictions of Refs. 2 and 3. Although substantial progress has been achieved in the detection of spin Hall effect, it should be noted that there are still intensive debates on whether intrinsic spin Hall effect does or can survive in a spin-orbit coupled system. For example, several recent theoretical works have argued that, except for the ballistic transport limit, intrinsic spin Hall effect cannot survive in a diffusive two-dimensional electron gas with Rashba spin-orbit coupling even in the weak impurity scattering limit.[9–15] As to the physical understanding of the recent experimental results,[7,8] some significant controversies also exist which need further clarification. For details please refer to Refs. 16–25.

In this paper, we investigate theoretically another kind of electric-field-induced edge spin accumulation phenomenon which might occur in a thin strip of a two-dimensional electronic (electron or hole) system. From the theoretical viewpoints, this phenomenon is essentially a *kinetic magnetoelectric effect*[26] due to boundary-confinement-induced spin-orbit coupling (which will be called *edge SO coupling* below). But very interestingly, it would manifest in a very similar manner as was conceived in a spin Hall effect. For example, the electric-field-induced edge spin accumulation in a thin two-dimensional electron gas (2DEG) strip due to this phenomenon will be polarized perpendicular to the 2DEG plane but along opposite directions at both edges of the strip, and in the weak impurity scattering limit (below a certain disorder strength), the edge spin accumulation will not decrease as the disorder strength increases, thus it can survive even in the diffusive transport regime. These features are very similar to the recently discovered intrinsic spin Hall effect, but the mechanisms involved in this phenomenon are very different from that of an intrinsic spin Hall effect from the theoretical points of view. The results obtained in the present paper might provide some new implications to the proper physical understanding of some recent experimental results.[7,8]

The paper is organized as follows: in Sec. II an edge SO coupling model describing the boundary-confinement-

 

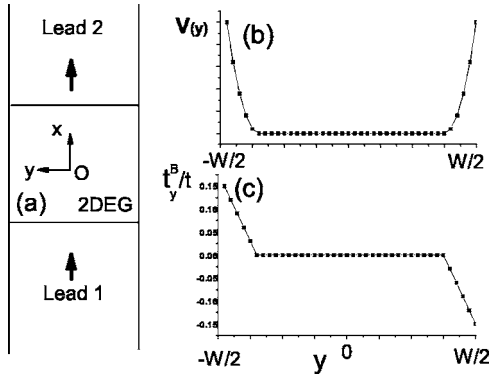


FIG. 1. (a) A two-dimensional (2D) semiconductor strip connected to two ideal leads. (b) Profile of the transverse spatial variation of the confining potential in the strip. (c) Profile of the transverse spatial variation of the spin-orbit coupling strength in the strip.

induced SO coupling in a thin 2DEG strip will be introduced and some details of the theoretical formalism used in our calculations will be briefly addressed, and in Sec. III some numerical results will be presented and discussed.

## II. MODEL AND THEORETICAL FORMULATION

The system considered in the present paper consists of a thin 2DEG strip connected to two ideal leads, as is shown in Fig. 1(a). The longitudinal direction of the strip will be defined as the $x$ direction, the transverse direction will be defined as the $y$ direction, and the normal of the 2DEG plane will be defined as the $z$ direction. According to the theory of the relativistic quantum mechanics, if the movement of an electron is confined by a spatially nonuniform potential, the spin and orbital degrees of freedom of the electron will be coupled together.[27] For the sake of simplification, we assume that the confining potential is spatially uniform along the longitudinal direction of the strip, i.e., the spatial variation of the confining potential occurs only in the transverse direction of the strip. Under this assumption, the SO coupling due to the transverse spatial variation of the confining potential will take the following form:[27,28]

$$\hat{H}_{SO} = -\frac{\hbar^2}{4m^2c^2}\hat{\sigma} \times \mathbf{k} \cdot \nabla V(y), \tag{1}$$

where $\hat{\sigma}=(\hat{\sigma}_x,\hat{\sigma}_y,\hat{\sigma}_z)$ are the usual Pauli matrices, $\mathbf{k}$ is the wave vector of electrons, $\nabla$ denotes the usual gradient operator, and $V(y)$ is the transverse confining potential, which is assumed to depend only on the $y$ coordinates. From the effective Hamiltonian (1) one can see that, for an electron moving to the $+x$ (or $-x$) direction, the SO coupling will tend to force the electron spin to align along the $+z$ (or $-z$) direction, depending on the sign of $\partial V(y)/\partial y$. In the absence of external electric fields, the numbers of electrons moving to the $+x$ and $-x$ directions are equal and hence no net spin density can be resulted from the SO coupling. However, if a longitudinal charge current circulates through the strip, the numbers of electrons moving to the $-x$ direction will be larger than the number of electrons moving to the $+x$ direction, hence a nonequilibrium spin density (polarized along the $+z$ or $-z$ direction, depending on the sign of $\partial V(y)/\partial y$) might result from the SO coupling. Such an effect had been dubbed the *kinetic magnetoelectric effect* in the literature.[26] For a 2DEG strip, if the strip width is much larger than the lattice constant, one can further assume that the confining potential $V(y)$ varies substantially only in a narrow boundary region as is shown in Fig. 1(b). (We assume that the two boundaries of the strip are located at $y=\pm\frac{W}{2}$). Then the SO coupling exists only near both edges of the strip, and due to the symmetry of the confining potential, the SO coupling coefficient (proportional to $\partial V(y)/\partial y$) will have opposite signs at both edges of the strip, as is shown in Fig. 1(c). Due to this fact, the electric-field-induced nonequilibrium spin density obtained based on this *edge SO coupling model* will be polarized perpendicular to the 2DEG plane but along opposite directions at both edges of the strip, similar to a spin Hall effect. This physical picture will be confirmed by detailed numerical calculations below. In order to make a comparison with the widely studied intrinsic spin Hall effect in a Rashba two-dimensional electron gas, we can also include a Rashba SO coupling term in our edge SO coupling model. Then the total Hamiltonian of the strip will be

$$\hat{H} = \frac{\hbar^2 k^2}{2m} + \alpha(\hat{\sigma} \times \vec{k}) \cdot \vec{z} - \frac{\hbar^2}{4m^2c^2}\hat{\sigma} \times \mathbf{k} \cdot \nabla V(y) + V(y), \tag{2}$$

where the second term denotes the Rashba SO coupling (which arises from the inversion asymmetry of the trapping well along the normal of the 2DEG plane), $\alpha$ is the Rashba SO coupling constant and $\vec{z}$ the unit vector along the normal of the 2DEG plane. A direct use of the Hamiltonian (2) is not convenient if one wants to take into account the effects of impurity scatterings properly, which are very important in the diffusive transport regime. So in our calculations we will transform the Hamiltonian (2) into a discrete form. The discrete version of the effective Hamiltonian for the total system (including both the leads and the 2DEG strip) will read,

$$\begin{aligned}\mathcal{H} = & -t\sum_{p=1,2}\sum_{\langle i,j\rangle\sigma}(C^{\dagger}_{p_i\sigma}C_{p_j\sigma} + \text{h.c.}) + \sum_{R_i}(\varepsilon_{R_i} + V_{R_i})\Psi^{\dagger}_{R_i}\Psi_{R_i} \\ & - t\sum_{\langle R_i,R_j\rangle}(\Psi^{\dagger}_{R_i}\Psi_{R_j} + \text{H.c.}) - t\sum_{p_n,R_n}(C^{\dagger}_{p_n\sigma}C_{R_n\sigma} + \text{H.c.}) \\ & - t^R\sum_{R_i}[i(\Psi^{\dagger}_{R_i}\sigma^x\Psi_{R_i+y} - \Psi^{\dagger}_{R_i}\sigma^y\Psi_{R_i+x}) + \text{H.c.}] \\ & - \sum_{R_i} t^B_{R_i}[i\Psi^{\dagger}_{R_i}\sigma^z\Psi_{R_i+x} + \text{H.c.}].\end{aligned} \tag{3}$$

Here $t=\hbar^2/2m^*a^2$ is the hopping matrix element between two nearest-neighbor lattice sites in the system, $m^*$ is the effective mass of electrons, and $a$ is the lattice constant. $\Psi_{R_i}=(C_{R_i\uparrow},C_{R_i\downarrow})$ is the annihilation operator of electrons at a lattice site $R_i$ in the strip. $C_{p_j\sigma}$ is the annihilation operator of electrons at a lattice site $p_j$ and with a spin $\sigma$ in the lead $p$ $(p=1,2)$. $(p_n,R_n)$ stands for a pair of nearest-neighbor lattice sites across the border between the strip and the lead $p$. In

the second term in Eq. (3), $\varepsilon_{R_i}$ denotes the on-site energy of free conduction electrons in the strip and $V_{R_i}$ the position-dependent confining potential depicted in Fig. 1(b). In a clean system without disorder, the on-site energy $\varepsilon_{R_i}$ is usually set to zero. The last two terms in Eq. (3) denote the Rashba SO coupling and the boundary-confinement-induced edge SO coupling in the strip, respectively, and $t_R=\alpha/2a$ is the Rashba SO coupling constant (which is assumed to be site independent) and $t_{R_i}^B=\frac{\hbar^2}{8m^{*2}c^2a}\frac{\partial V}{\partial y}$ is the edge SO coupling constant (which is site dependent). The site dependence of $t_{R_i}^B$ will be determined by the actual form of the transverse confinement potential shape in the strip. In our calculations we will assume a parabolic confining potential near both edges of the strip, as is shown in Fig. 1(b). In such cases, the site dependence of the edge SO coupling constant can be expressed as

$$t_{R_i}^B = \pm t^B \max(N_B + |y| - N_y/2, 0), \tag{4}$$

where $N_y$ is the width of the strip (in units of the lattice constant), $N^B$ is the width of the narrow boundary region in which the edge SO coupling exists, and $t^B$ is the minimum value of the site-dependent edge SO coupling constant. (After $t^B$ and $N^B$ are given, the position dependence of the parabolic confining potential will also be determined.) As is shown in Fig. 1(c), the edge SO coupling constant should have opposite signs at both edges of the strip.

Our calculations will be based on the usual Landauer-Büttiker formulation.[29] But unlike the usual Landauer-Büttiker formula, where all one needs are usually only the scattering amplitudes between different leads, for the problem studied in the present paper one must also find out explicitly the electron wave functions inside the strip in order to calculate the electric-field-induced nonequilibrium spin density in the strip. To this end, we will start by considering the transmission of an incident wave from a lead.[30] The real space wave function of an incident electron from a lead $p$ and with a spin $\sigma$ will be denoted as $e^{-ik_m^p x_p}\chi_{m\sigma}^p(y_p)$, where $\chi_{m\sigma}^p(y_p)$ denotes the $m$th transverse mode in the lead $p$ and with the spin $\sigma$, and $k_m^p$ denotes the longitudinal wave vector. We adopt the local coordinate scheme for all leads. In the local coordinate scheme, the longitudinal coordinate $x_q$ in the lead $q$ will take the integer numbers $1,2,\ldots,\infty$ away from the border between the lead and the strip, and the transverse coordinate $y_q$ will take the value of $-N_q/2,\ldots,N_q/2$. The longitudinal wave vector $k_m^p$ satisfies the relation $-2t\cos(k_m^p)+\varepsilon_m^p=E$, where $\varepsilon_m^p$ is the eigenenergy of the $m$th transverse mode in the lead $p$ and $E$ the energy of the incident electron. Corresponding to an incident wave from the $(m\sigma)$ channel in the lead $p$, the transmitted wave in the lead $q$ can be expressed as $\psi^{pm\sigma}(x_q,y_q)=\Sigma_{\sigma'}\psi_{\sigma'}^{pm\sigma}(x_q,y_q)|\sigma'\rangle$ ($|\sigma'\rangle=|\uparrow\rangle$ or $|\downarrow\rangle$), where $\psi_{\sigma'}^{pm\sigma}(x_q,y_q)$ has the following general form:

$$\psi_{\sigma'}^{pm\sigma}(x_q,y_q) = \delta_{pq}\delta_{\sigma\sigma'}e^{-ik_m^p x_p}\chi_{m\sigma}^p(y_p) + \sum_n \phi_{qn\sigma'}^{pm\sigma}e^{ik_n^q x_q}\chi_{n\sigma'}^q(y_q), \tag{5}$$

in which $\phi_{qn\sigma'}^{pm\sigma}$ stands for the scattering amplitude from the $(m\sigma)$ channel in the lead $p$ to the $(n\sigma')$ channel in the lead $q$. (Due to the presence of the SO coupling in the scattering region (i.e., in the strip), the spin is not a conserved quantity when an electron incident from a lead $p$ is transmitted to another lead $q$.) The scattering amplitudes $\phi_{qn\sigma'}^{pm\sigma}$ will be obtained by solving the Schrödinger equation for the entire system, which has now a lattice form and hence there is *a separate equation* for each lattice site and spin index. Since Eq. (5) is a linear combination of all outgoing modes with the same energy $E$ in the lead $q$, the Schrödinger equation is satisfied automatically in the lead $q$, except for the lattice sites in the *first row* (i.e., $x_q=1$) of the lead that are connected directly to the strip. Due to the coupling between the leads and the strip, the lattice form of the Schrödinger equation for the lattice sites in the *first* row of a lead are different from that for other lattice sites in the lead and hence cannot be satisfied automatically by Eq. (5). Due to this reason, the wave function at the lattice sites in the first row of a lead (which are determined by the scattering amplitudes $\phi_{qn\sigma'}^{pm\sigma}$) must be solved with the wave function in the strip simultaneously. Corresponding to an incident wave from the $(m\sigma)$ channel in the lead $p$, in the presence of the edge SO coupling, the wave function $\psi^{pm\sigma}(R_i)$ in the strip will be a superposition of a spin-up and a spin-down component, which can be expressed as

$$\psi^{pm\sigma}(R_i) = \sum_{\sigma'} \psi_{\sigma'}^{pm\sigma}(R_i)|\sigma'\rangle, \tag{6}$$

where $|\sigma'\rangle=|\uparrow\rangle$ (spin-up) or $|\downarrow\rangle$ (spin-down). From the Hamiltonian (3), one can show that the lattice form of the Schrödinger equation for the lattice sites in the strip and for the lattice sites in the *first* row of a lead $p'$ connected directly to the strip will have the following form:

$$E\psi_{\sigma'}^{pm\sigma}(\mathbf{r}_s) = \sum_{\mathbf{r}_s',\sigma''} H_{strip}(\mathbf{r}_s\sigma',\mathbf{r}_s'\sigma'')\psi_{\sigma''}^{pm\sigma}(\mathbf{r}_s') - t\sum_{p',y_{p'}} \delta_{\mathbf{r}_s,\mathbf{n}(p',y_{p'})}\psi_{\sigma'}^{pm\sigma}(1,y_{p'}'), \tag{7}$$

$$E\psi_{\sigma'}^{pm\sigma}(\mathbf{x}_{p'}')_{\mathbf{x}_{p'}'=(1,y_{p'}')} = \sum_{\mathbf{x}_{p'}''} H_{lead}(\mathbf{x}_{p'}',\sigma',\mathbf{x}_{p'}'',\sigma')\psi_{\sigma'}^{pm\sigma}(\mathbf{x}_{p'}'') - t\sum_{\mathbf{r}_s} \delta_{\mathbf{r}_s,n(p',y_{p'})}\psi_{\sigma'}^{pm\sigma}(\mathbf{r}_s), \tag{8}$$

where $(\mathbf{r}_s,\mathbf{r}_s')$ denote two nearest-neighbor lattice sites in the strip and $(\mathbf{x}_{p'}',\mathbf{x}_{p'}'')$ two nearest-neighbor lattice sites in the lead $p'$, respectively, and for clarity, we have also used explicitly a double index $(1,y_{p'}')$ to denote a lattice site in the first row (i.e., $x_{p'}'=1$) of the lead $p'$ and used $\mathbf{n}(p',y_{p'})$ to denote a boundary lattice site in the strip connected directly to the lattice site $(1,y_{p'}')$ in the first row of the lead $p'$. The first terms in Eqs. (7) and (8) describe the coupling between two nearest-neighbor lattice sites both in the strip or both in the lead $p'$, respectively. The second terms in them arise from the coupling between the strip and the lead $p'$. To make the meanings of these two kinds of terms more explicit, in Eqs. (7) and (8) we have used $H_{strip}(\mathbf{r}_s\sigma',\mathbf{r}_s'\sigma'')$ to denote the

Hamiltonian for an *isolated* strip (i.e., without the coupling to the leads) and used $H_{lead}(\mathbf{x}'_{p'},\sigma',\mathbf{x}''_{p'},\sigma')$ to denote the Hamiltonian for an *isolated* lead $p'$ (i.e., without the coupling to the strip), respectively, whose matrix elements can be written down directly from Eq. (3).

Eqs. (7) and (8) are the match conditions for the wave functions in the strip and in the leads. To express the match conditions in a more compact form, we define the wave function $\psi^{pm\sigma}_{\sigma'}(R_i)$ in the strip as a column vector $\Psi$ whose dimension is $2N$ ($N$ is the total number of lattice sites in the strip). The scattering amplitudes $\phi^{pm\sigma}_{qn\sigma'}$ will be arranged into another column vector $\Phi$ whose dimension is $2M$ ($M$ is the total number of lattice sites in the first row of a lead). Substituting Eq. (5) into Eqs. (7) and (8) and then making use of the orthogonality relations for the transverse modes in the leads (i.e., $\Sigma_{y_2}\chi^q_{n\sigma}(y_2)\chi^q_{n'\sigma'}(y_2)=\delta_{nn'}\delta_{\sigma\sigma'}$), we arrive at the following matrix equations for the unknown column vectors $\Psi$ and $\Phi$:

$$\mathbf{A}\Psi = \mathbf{b} + \mathbf{B}\Phi, \quad \mathbf{C}\Phi = \mathbf{d} + \mathbf{D}\Psi, \tag{9}$$

where $\mathbf{A}$ and $\mathbf{C}$ are two square matrices with a dimension of $2N\times 2N$ and $2M\times 2M$, respectively; $\mathbf{B}$ and $\mathbf{D}$ are two rectangular matrices describing the coupling between the leads and the strip; $\mathbf{b}$ and $\mathbf{d}$ are two column vectors describing the contributions from the incident waves. Some details of these matrices and column vectors are given in the Appendix. From Eq. (9) both the scattering amplitudes $\phi^{pm\sigma}_{qn\sigma'}$ and the wave function $\psi^{pm\sigma}_{\sigma'}(R_i)$ in the strip can be obtained simultaneously. After obtaining all scattering amplitudes $\phi^{pm\sigma}_{qn\sigma'}$ from Eq. (9), we can calculate the charge current in each lead through the Landauer-Büttiker formula, $I_p=(e^2/h)\Sigma_q\Sigma_{\sigma_1,\sigma_2}(T^{q\sigma_1}_{p\sigma_2}V_q-T^{p\sigma_2}_{q\sigma_1}V_p)$, where $V_q=\mu_q/(-e)$ is the voltage applied in the lead $q$ and $\mu_q$ is the chemical potential in the lead $q$, and $T^{p\sigma}_{q\sigma'}$ are the transmission probabilities defined by $T^{p\sigma}_{q\sigma'}=\Sigma_{m,n}|\phi^{pm\sigma}_{qn\sigma'}|^2 v_{qn}/v_{pm}$ and $v_{pm}=2t\sin(k^p_m)$ is the longitudinal velocity of the $m$th transverse mode in the lead $p$. The spin current in each lead can be calculated similarly, with $I^{\sigma}_p=-(e/4\pi)\Sigma_q\Sigma_{\sigma_2}[(T^{q\sigma_2}_{p\sigma}-T^{q\sigma_2}_{p\bar{\sigma}})V_q-(T^{p\sigma}_{q\sigma_2}-T^{p\bar{\sigma}}_{q\sigma_2})V_p]$.

After the wave function $\psi^{pm\sigma}_{\sigma'}(R_i)$ in the strip is obtained by solving Eq. (9), the spin density in the strip can also be calculated readily by taking proper ensemble average.[29] For this purpose, one should first normalize the wave function by a factor of $1/\sqrt{L}$ ($L\to\infty$ is the length of the lead) so that there is one particle associated with each incident wave[29] (corresponding to that the longitudinal part $e^{-ik^p_m\sigma}$ of an incident wave from a lead $p$ is normalized to $e^{-ik^p_m\sigma}/\sqrt{L}$). Then for an electron incident from the $(m\sigma)$ channel in the lead $p$ [the corresponding wave function in the strip is given by Eq. (6)], the $\alpha$ component of the position-dependent spin expectation value in the strip will be given by

$$\vec{S}_\alpha(R_i) = (1/L)\sum_{\sigma',\sigma''}\psi^{pm\sigma *}_{\sigma'}(R_i)\vec{\sigma}^{\alpha}_{\sigma',\sigma''}\psi^{pm\sigma}_{\sigma''}(R_i), \tag{10}$$

where $\vec{\sigma}^{\alpha}_{\sigma',\sigma''}=\langle\sigma'|\hat{\sigma}_\alpha|\sigma''\rangle$ ($\alpha=x,y,z$). The net spin density will be obtained by summing over all incident channels with the corresponding densities of states. The density of states corresponding to the $(m\sigma)$ channel in the lead $p$ will be given by $\frac{L}{2\pi}\frac{dk}{dE}=\frac{L}{2\pi\hbar v_{pm}}$, where $v_{pm}=2t\sin(k^p_m)$ is the longitudinal velocity of the $m$th transverse mode in the lead $p$. In the linear transport regime, only those channels close to the Fermi level will contribute to the summation,[29] hence the result can be expressed explicitly as

$$\langle\vec{S}_\alpha(R_i)\rangle = \frac{1}{2\pi}\sum_{pm\sigma}\mu_p/\hbar v_{pm}\sum_{\sigma',\sigma''}\psi^{pm\sigma *}_{\sigma'}(R_i)\vec{\sigma}^{\alpha}_{\sigma',\sigma''}\psi^{pm\sigma}_{\sigma''}(R_i), \tag{11}$$

where $\langle\vec{S}_\alpha(R_i)\rangle$ denotes the net spin density at the site $R_i$ in the strip and $\mu_p$ the chemical potential in the lead $p$.

## III. RESULTS AND DISCUSSIONS

In our calculations we will take the typical values of the electron effective mass $m^*=0.04m_e$ and the lattice constant $a=3$ nm.[31] The chemical potentials in the leads will be set by fixing the longitudinal charge current density to the experimental value ($\approx 100\ \mu$A/1.5 $\mu$m) as reported in Ref. 8. The Fermi energy of the 2DEG strip will be set to $E_f=-3.8t$ throughout the calculations.

In Fig. 2(a) we show the typical patterns of the spatial distribution of the electric-field-induced nonequilibrium spin density $\langle S_z\rangle$ in the 2DEG strip obtained based on the edge SO coupling model. (Other components of the spin density are zero for the case of the edge SO coupling model, which are not shown in the figure.) We have used $180\times 60$ lattice sites in total (including both the leads and the 2DEG strip) in the calculations and the strip contains $60\times 60$ lattice sites. From Fig. 2(a) one can see that the spatial distribution of the electric-field-induced nonequilibrium spin density in the 2DEG strip obtained based on the edge SO coupling model manifests in a very similar form as was conceived in a spin Hall effect,[7,8] i.e., the nonequilibrium spin density is polarized perpendicular to the 2DEG plane but along opposite directions at both edges of the strip and the spin density has two opposite extrema near both edges. By fixing the longitudinal charge current density to the experimental value ($\approx 100\ \mu$A/1.5 $\mu$m) as reported in Ref. 8 and setting the edge SO coupling coefficient to $t^B\simeq 0.03t$, we found that the nonequilibrium spin polarization near both edges of the strip obtained based on this edge SO coupling model has roughly the same order of magnitude ($\approx 1\%$) as the corresponding experimental values reported in Ref. 8. To make a comparison with the widely studied two-dimensional (2D) Rashba SO coupling model,[16] in Fig. 2(b) we have also plotted the spatial distribution of the electric-field-induced nonequilibrium spin density $\langle S_z\rangle$ in the 2DEG strip obtained based on the usual Rashba SO coupling model. From Figs. 2(a) and 2(b) one can see that, the typical patterns of the spatial distributions of the electric-field-induced nonequilibrium spin density $\langle S_z\rangle$ are very similar in both cases. But it should be pointed out that, for the case of our edge SO coupling model, only the $z$ component of the spin density is nonzero, but for the case of the usual Rashba SO coupling model, all three

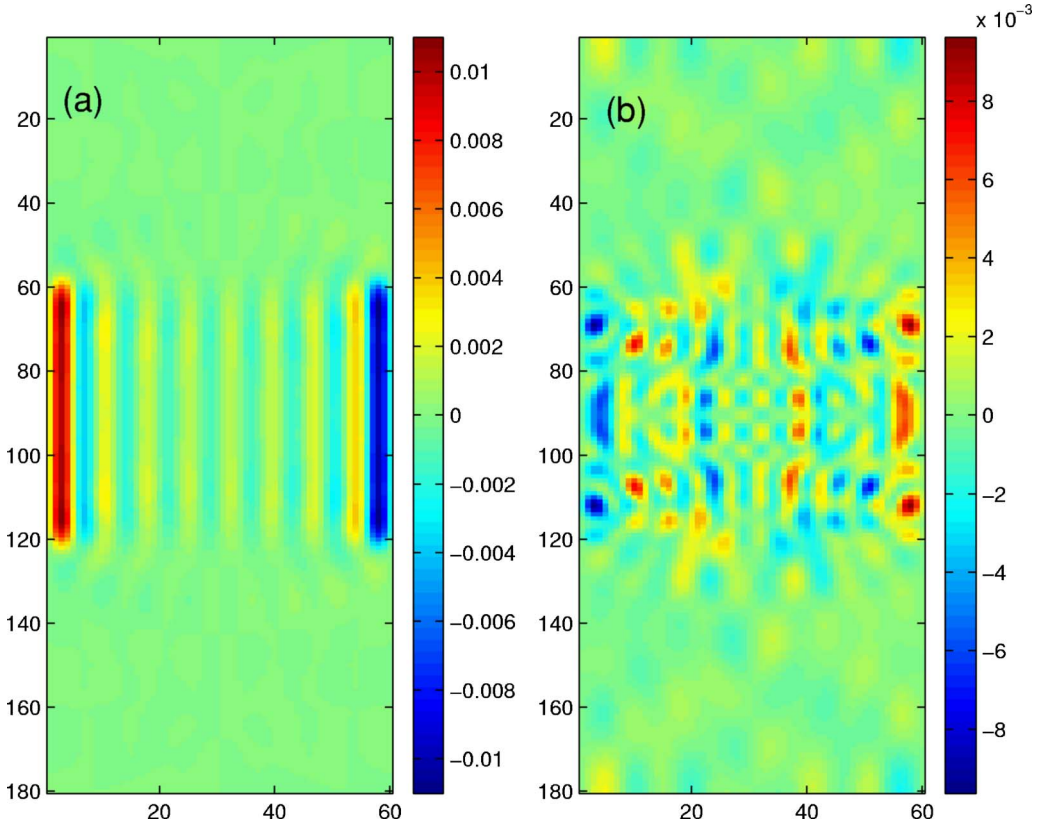


FIG. 2. (Color online) The two-dimensional real space configuration of the electric-field-induced nonequilibrium spin density $\langle S_z(x,y)\rangle$ (in units of $\hbar/2$) in the 2DEG strip obtained based on (a) the edge SO coupling model and (b) the Rashba SO coupling model, resepctively. In Fig. 1(a) the Rashba SO coupling constant is set to be zero and the edge SO coupling constant is set to be $t^B=0.03t$. The width of the boundary region in which the edge SO coupling exists is set to be $N^B=5$. In Fig. 1(b) the Rashba SO coupling constant is set to be $t_R=0.15t$ and the edge SO coupling constant is set to zero. In both cases, the strip contains $60\times 60$ lattice sites.

components of the spin density are nonzero. (In Fig. 2(b) we have plotted only the spatial distribution of the $z$ component of the spin density for comparison.) Another slight difference that can be seen from Figs. 2(a) and 2(b) is that, the transverse spatial distribution of the spin density has a very regularly striped pattern in the case of the edge SO coupling model, but for the case of the usual Rashba SO coupling model, the spin-density pattern is not much regularly striped. This slight difference arises from the fact that, in the case of our edge SO coupling model, the SO coupling exists only in a narrow boundary region near both edges of the strip [see the illustration shown in Figs. 1(b) and 1(c)] and the spatial distribution of the spin-orbit coupling constants was assumed to be uniform along the longitudinal direction of the strip. These assumptions lead to a regularly striped spin-density pattern as shown in Fig. 2(a). For the case of the usual Rashba SO coupling model, the SO coupling exists in the entire strip (i.e., the SO coupling constant is nonzero everywhere inside the strip), thus the spin-density pattern in the strip is not much regularly striped.

In Figs. 3(a)–3(d) we show the variations of the electric-field-induced nonequilibrium spin polarization and its transverse spatial distribution in the 2DEG strip as the strip width increases obtained based on the edge SO coupling model, and in Fig. 3(e) we show the variations of the nonequilibrium spin polarization and its transverse spatial distribution in the strip as the edge SO coupling strength varies. Because the spatial distribution of the nonequilibrium spin density has a regularly striped pattern along the longitudinal direction of the strip, in Figs. 3(a)–3(e) we use an averaged value of $\langle S_z(x,y)\rangle$, defined by $\langle S_z(y)\rangle=\frac{1}{L}\int_0^L S_z(x,y)dx$, as a measure of the nonequilibrium spin polarization. From Figs. 3(a)–3(e) one can see that $\langle S_z(y)\rangle$ oscillates inside the strip but has opposite signs at both edges of the strip, and the magnitude of the spin polarization will reach a maximum value (denoted as $S^z_{max}$ below) near both edges of the strip. From the theoretical points of view, this oscillation is a natural result of the quantum interference between the spin-up and spin-down components of the electron wave functions inside the strip. (In the presence of the edge SO coupling, the electron wave function inside the strip is inherently a superposition of the spin-up and spin-down components. See Eqs. (6), (10), and (11) and the explanations given to them. For the case of a 2D semiconductor strip with Rashba SO coupling, similar oscillations can also be predicted, see, e.g., the discussions in Ref. 22.) From Figs. 3(a)–3(d) one can see that, the oscillation of the spin polarization inside the strip is substantial if the width of the boundary region in which the SO coupling exists is comparable to the total width of the strip. But if the width of this boundary region is much smaller than the total width of the strip, the oscillation will decay substantially inside the strip, i.e., the spin accumulation will be localized near both edges of the strip. On the other hand, from Fig. 3(e) one can see that the profiles of the transverse spatial

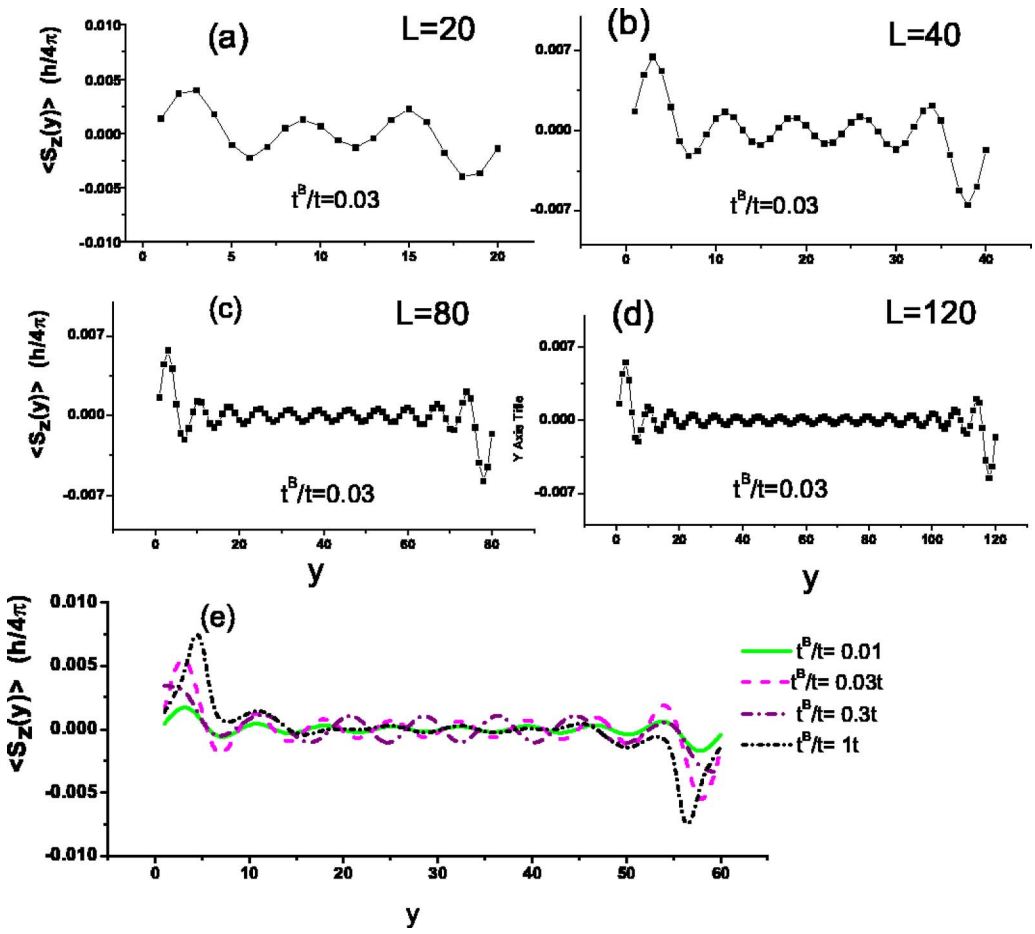


FIG. 3. (Color online) Illustration of the variations of the transverse spatial distribution of the longitudinally averaged spin density $\langle S_z(y)\rangle$ inside the strip as the strip width increases obtained based on the edge SO coupling model. The lattice sizes of the strip are chosen as: (a) $20\times20$, (b) $40\times40$, (c) $80\times80$, and (d) $120\times120$. The edge SO coupling constant is set to be $t^B=0.03t$. Figure 3(e) shows the changes of the transverse spatial distribution of $\langle S_z(y)\rangle$ inside the strip as the edge SO coupling strength varies, where the lattice size is fixed to be $60\times60$. In all calculations, the width of the boundary region in which the edge SO coupling exists is set to be $N^B=5$.

distribution of the spin polarization do not change substantially as the edge SO coupling strength varies. From these figures one can also note that, the order of the magnitude of the spin polarization near both edges of the strip remains almost unchanged as the strip width increases, suggesting that the electric-field-induced edge spin accumulation due to boundary-confinement-induced edge SO coupling in a 2D semiconductor strip may survive even in the diffusive transport regime, similar to the phenomenon reported in Ref. 8. (For a 2D semiconductor strip with Rashba spin-orbit coupling, it was generally believed that the intrinsic spin Hall effect cannot survive in the diffusive transport regime[9–15].)

Finally, we discuss the effects of random impurity scatterings on the electric-field-induced nonequilibrium spin accumulation in the case of the edge SO coupling model. To include properly the effects of random impurity scatterings, we assume that the on-site energy $w_{R_i}$ in the 2DEG strip is randomly but uniformly distributed in an energy region $[-W_D, W_D]$, where $W_D$ is the amplitude of the on-site energy fluctuations, which characterizes the disorder strength.[17,18] We will calculate the spin density for a number of random impurity configurations and then do an impurity average. In Figs. 4(a) and 4(b) we show the variations of the edge spin accumulation ($S^z_{max}$) as the disorder strength increases for the cases of both the edge SO coupling model and the usual Rashba model, respectively. We have done an impurity average over 10 000 random impurity configurations for each case. From Fig. 4(a) one can see that, for the case of the edge SO coupling model, the edge spin accumulation does not decrease as the disorder strength increases in the weak impurity scattering limit (i.e., below a certain disorder strength) and for a fixed longitudinal change current density ($\approx$100 $\mu$A/1.5 $\mu$m), similar to the intrinsic spin Hall effect reported in Ref. 8. In contrast, for the case of the usual Rashba model, the edge spin accumulation decreases monotonously as the disorder strength increases even in the weak impurity scattering limit, which can be seen clearly from Fig. 4(b). The different behaviors in these two models can be understood qualitatively as follows. For the case of the edge SO coupling model, the SO coupling exists only in a narrow boundary region near both edges of the strip [see the illustration shown in Figs. 1(b) and 1(c)]. The electric-field-induced nonequilibrium spin density in this model is due to the kinetic magnetoelectric effect but not due to the flow of a transverse spin Hall current, thus only those scattering events occurring near both edges of the strip will af-

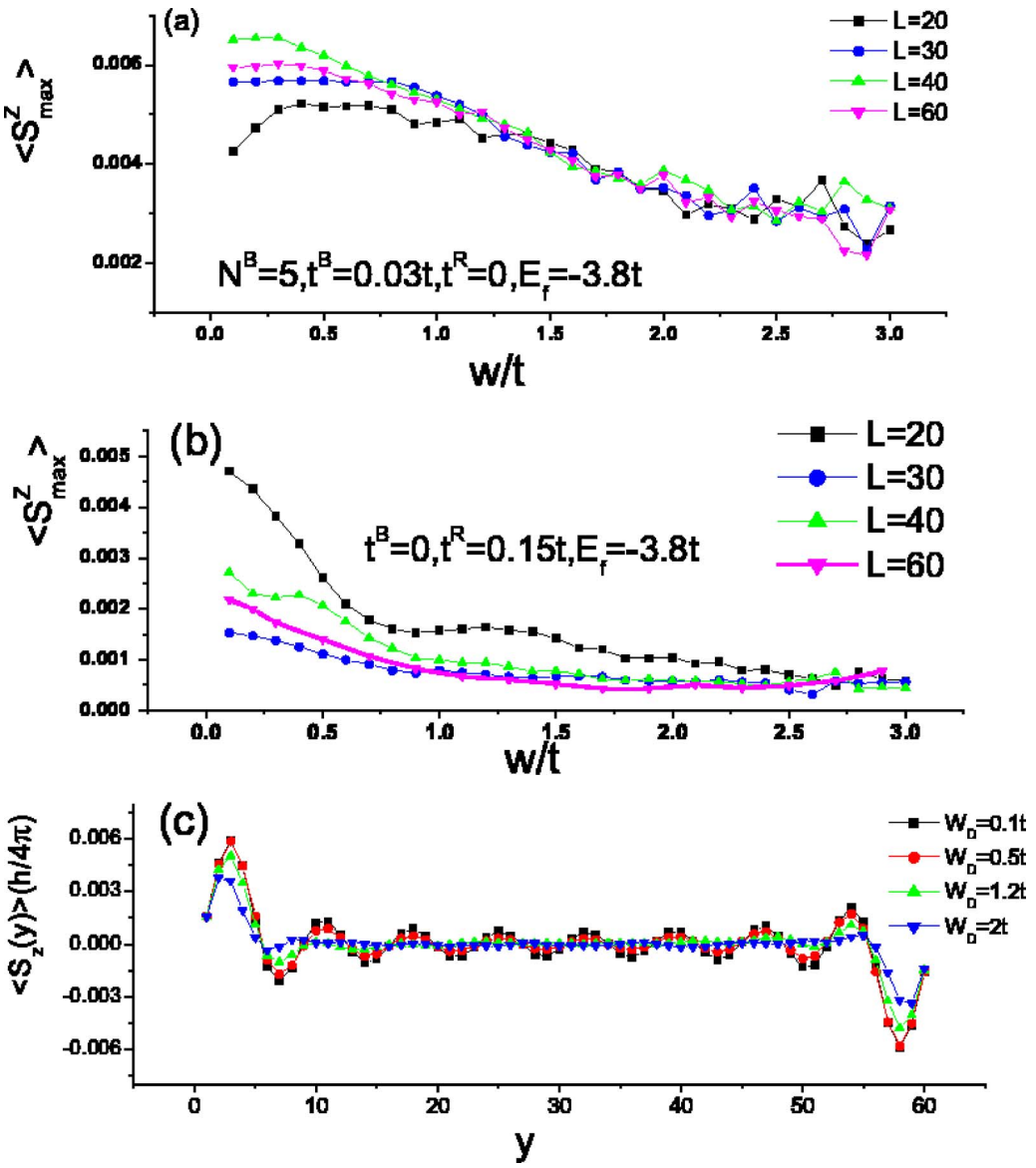


FIG. 4. (Color online) (a) Plot of the edge spin accumulation ($\langle S^z_{max}\rangle$) versus the disorder strength ($W_D$) obtained based on the edge SO coupling model. (b) Plot of the edge spin accumulation ($\langle S^z_{max}\rangle$) versus the disorder strength ($W_D$) obtained based on the Rashba SO coupling model. (c) The transverse spatial distribution of the nonequilibrium spin density inside the strip in the presence of disorder. (The parameters used in the calculations are shown in the figures.)

fect substantially the spin density. In contrast, for the case of the usual Rashba model, the electric-field-induced nonequilibrium spin density is due to the flow of a transverse spin Hall current,[16] which will be dampened significantly by all the random impurity scattering events occurring in the entire strip and hence the edge spin accumulation will be decreased substantially with increasing disorder strength even in the weak impurity scattering limit. Of course, because localization effects will become important in the presence of strong impurity scatterings, the electric-field-induced nonequilibrium spin density in the case of the edge SO coupling model will also be decreased substantially in the presence of strong impurity scatterings, which can be seen clearly from Fig. 4(a). Finally, in Fig. 4(c) we show the effects of random impurity scatterings on the transverse spatial distribution of the nonequilibrium spin polarization in the strip obtained based on the edge SO coupling model. From Fig. 4(c) one can see that, compared with the cases shown in Fig. 3, the oscillations of the spin polarization inside the strip will be suppressed substantially in the presence of random impurity scatterings. From the theoretical points of view, the random impurity scatterings will destroy significantly the quantum interference effect of the spin-up and spin-down components of the electron wave functions inside the strip and therefore suppress substantially the oscillation of the spin polarization inside the strip.

In summary, we have presented a microscopic model calculation for the kinetic magnetoelectric effect in a thin strip of a two-dimensional electronic system due to boundary-confinement-induced edge SO coupling. We have shown that this effect can manifest in a very similar form as was conceived in a spin Hall effect and some important features of

this effect are similar to the recently discovered intrinsic spin Hall effect in thin strips of two-dimensional $p$-doped semiconductors.[8] The results obtained in the present paper might provide some new implications to the proper understanding of the effects of boundary conditions in some recently observed experimental phenomena. However, it should be stressed that these results are obtained based on a more ideal theoretical model and the effects discussed are very sensitive to the edge spin-orbit coupling parameters and the edge confinement potential shape. For interpreting the real experiments, one needs to use the actual values of the edge spin-orbit coupling parameters and must consider the actual form of the edge confinement potential shape. A strict treatment of these factors is beyond the scope of the approach developed in the present paper.

*Note added in proof.* Recently, we became aware of a recent work by Y. X. Xing, Q. F. Sun, L. Tang, and J. P. Hu,[32] where a similar edge spin-orbit coupling model was considered.

## ACKNOWLEDGMENTS

Y. J. Jiang was supported by the Natural Science Foundation of Zhejiang Province (Grant No. Y605167). L. B. Hu was supported by the National Science Foundation of China (Grant No. 10474022) and the Natural Science Foundation of Guangdong Province (Grant No. 05200534).

## APPENDIX: SOME DETAILS FOR THE MATRICES IN EQ. (9)

In this appendix we give some details for the matrices $\mathbf{A},\mathbf{B},\mathbf{C},\mathbf{D}$ and the column vectors $\mathbf{b}$ and $\mathbf{d}$ in Eq. (9). The matrix $\mathbf{A}$ in Eq. (9) is given by $\mathbf{A}=E\mathbf{I}-\mathbf{H}_{strip}$, where $\mathbf{I}$ stands for the unit matrix. The elements for the matrices $\mathbf{B},\mathbf{C},\mathbf{D}$ and the column vectors $\mathbf{b}$ and $\mathbf{d}$ can be given explicitly by

$$\mathbf{B}(n_{p''y}\sigma'',p'm'\sigma') = -\delta_{p'',p'}\delta_{\sigma'',\sigma'}t\chi^{p'}_{m'}(y_{p''})e^{ik^{p'}_{m'}},$$

$$\mathbf{D}(p'm'\sigma',n_{p''y}\sigma'') = -\delta_{p'',p'}\delta_{\sigma'',\sigma'}t\chi^{p'}_{m'}(y_{p''}),$$

$$\mathbf{C}(p'm'\sigma',p''m''\sigma'') = -\delta_{p'',p'}\delta_{\sigma'',\sigma'}\delta_{m''m'}t,$$

$$\mathbf{b}(n_{p'y}\sigma') = -\delta_{pp'}\delta_{\sigma\sigma'}t\chi^{p}_{m}(y_{p'})e^{-ik^{p}_{m}},$$

$$\mathbf{d}(p'm'\sigma') = \delta_{pp'}\delta_{mm'}\delta_{\sigma\sigma'}t,$$

where for simplicity of notation we have used simply a symbol $n_{p'y}$ to denote a boundary lattice site $\mathbf{n}(p',y_{p'})$ in the strip connected directly to a lattice site $(1,y'_{p'})$ in the *first row* of the lead $p'$. [See the explanations in the text given to Eqs. (7) and (8)]. The indices for leads, transverse modes, lattice sites, and spins can take all possible values. All other matrix elements not shown explicitly above are zero.

[1] J. E. Hirsch, Phys. Rev. Lett. **83**, 1834 (1999); S. Zhang, *ibid.* **85**, 393 (2000).
[2] S. Murakami, N. Nagaosa, and S. C. Zhang, Science **301**, 1348 (2003).
[3] J. Sinova, D. Culcer, Q. Niu, N. A. Sinitsyn, T. Jungwirth, and A. H. MacDonald, Phys. Rev. Lett. **92**, 126603 (2004).
[4] I. Zutic, J. Fabian, and S. Sarma, Rev. Mod. Phys. **76**, 323 (2004).
[5] D. Awschalom, D. Loss, and N. Samarth, *Semiconductor Spintronics and Quantum Computation* (Springer, Berlin, 2002).
[6] I. Dyakonov and V. I. Perel, Sov. Phys. JETP **33**, 467 (1971).
[7] Y. K. Kato, R. C. Myers, A. C. Gossard, and D. D. Awschalom, Science **306**, 5703 (2004).
[8] J. Wunderlich, B. Kaestner, J. Sinova, and T. Jungwirth, Phys. Rev. Lett. **94**, 047204 (2005).
[9] J. I. Inoue, G. E. W. Bauer, and L. W. Molenkamp, Phys. Rev. B **70**, 041303(R) (2004).
[10] E. G. Mishchenko, A. V. Shytov, and B. I. Halperin, Phys. Rev. Lett. **93**, 226602 (2004).
[11] E. I. Rashba, Phys. Rev. B **68**, 241315(R) (2003); Phys. Rev. B **70**, 201309(R) (2004).
[12] R. Raimondi and P. Schwab, Phys. Rev. B **71**, 033311 (2005).
[13] O. V. Dimitrova, Phys. Rev. B **71**, 245327 (2005).
[14] S. Zhang and Z. Yang, Phys. Rev. Lett. **94**, 066602 (2005).
[15] A. Khaetskii, Phys. Rev. Lett. **96**, 056602 (2006).
[16] B. K. Nikolic, S. Souma, L. P. Zarbo, and J. Sinova, Phys. Rev. Lett. **95**, 046601 (2005).
[17] B. K. Nikolic, L. P. Zarbo, and S. Souma, Phys. Rev. B **72**, 075361 (2005); *ibid.* **73**, 075303 (2006).
[18] L. Sheng, D. N. Sheng, and C. S. Ting, Phys. Rev. Lett. **94**, 016602 (2005); Q. Wang, L. Sheng, and C. S. Ting, cond-mat/0505576 (unpublished).
[19] A. G. Malshukov, L. Y. Wang, C. S. Chu, and K. A. Chao, Phys. Rev. Lett. **95**, 146601 (2005).
[20] H. A. Engel, B. I. Halperin, and E. I. Rashba, Phys. Rev. Lett. **95**, 166605 (2005).
[21] W. K. Tse and S. Das Sarma, Phys. Rev. Lett. **96**, 056601 (2006).
[22] A. Reynoso, G. Usaj, and C. A. Balseiro, Phys. Rev. B **73**, 115342 (2006).
[23] V. M. Galitski, A. A. Burkov, and S. Das Sarma, cond-mat/0601677 (unpublished).
[24] X. H. Ma, L. B. Hu, R. B. Tao, and S.-Q. Shen, Phys. Rev. B **70**, 195343 (2004); L. B. Hu, J. Gao, and S.-Q. Shen, *ibid.* **70**, 235323 (2004).
[25] Y. J. Jiang, cond-mat/0510664 (unpublished).
[26] V. M. Edelstein, Solid State Commun. **73**, 233 (1990).
[27] E. Merzbacher, *Quantum Mechanics* (Wiley, New York, 1998).
[28] R. Winkler, *Spin-Orbit Coupling Effects in Two Dimensional Electron and Hole Systems* (Springer, Berlin, 2003).
[29] S. Datta, *Electronic Transport in Mesoscopic Systems* (Cambridge University Press, Cambridge, 1997).
[30] Y. J. Jiang and L. B. Hu, cond-mat/0605361 (unpublished).
[31] J. Nitta, T. Akasaki, and H. Takayanagi, Phys. Rev. Lett. **78**, 1335 (1997).
[32] Y. X. Xing, Q. F. Sun, L. Tang, and J. P. Hu, cond-mat/0604502.